AD-A070 335 STANFORD UNIV CALIF EDWARD L GINZTON LAB F/G 9/5
PIEZOELECTRIC SHEAR SURFACE WAVE GRATING RESONATORS, (U)
MAY 77 B A AULD, B YEH N00014-75-C-0632
UNCLASSIFIED GL-2708 NL

1 OF 1
AD
A070335

END
DATE
FILMED
7-79
DDC

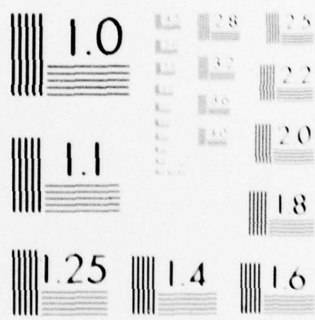


MICROCOPY RESOLUTION TEST CHART
NATIONAL BUREAU OF STANDARDS-1963-A

LEVEL

(2)

(6) PIEZOELECTRIC SHEAR SURFACE WAVE GRATING RESONATORS

by

(10) B. A. Auld and Bing-Hui Yeh





(14) GL-
G. L. Report No. 2708

(11) May 1977

(12) 8p.

To appear in

Proceedings of the 31st Annual

Symposium on Frequency Control

1977

Supported by the Joint Services Electronics

Program under Contract N00014-75-C-0632

(15)



Edward L. Ginzton Laboratory
W. W. Hansen Laboratories of Physics
Stanford University
Stanford, California

409 640 LB

Atlantic City, 1-3 June 1977

# PIEZOELECTRIC SHEAR SURFACE WAVE GRATING RESONATORS

B. A. Auld and Bing-Hui Yeh
Edward L. Ginzton Laboratory
W. W. Hansen Laboratories of Physics
Stanford University
Stanford, California

## Summary

This paper describes a new type of surface acoustic wave grating resonator in which the particle displacement of the surface wave is parallel to the surface. By contrast, the now well-known SAW (Rayleigh wave) grating resonator has its particle displacement in the saggital plane.

In the SAW resonator the function of the grating structure, which consists of either grooves or metal strips, is to provide two highly reflecting Rayleigh wave mirrors, between which a standing wave is excited by means of an interdigital transducer. The basic function of the grating in the horizontal shear (SH) type of surface wave resonator considered here is quite different. An SH surface wave cannot exist on a homogeneous (unlayered) substrate in the absence of some periodic variation, such as a grating, along the surface. That is to say, the surface wave in this case is a vibrational mode of the grating itself. On the other hand, the grating is now not required to realize a highly reflecting mirror, because the SH motion reflects without spurious mode coupling at a traction-free boundary placed in any symmetry plane of the structure. For this reason this new type of resonator promises a substantial advantage in miniaturization compared with the conventional SAW resonator.

SH surface wave resonators on PZT-8, Y-cut X-propagating $LiNbO_3$ and ST quartz have been fabricated and tested. Excitation was by means of an interdigital structure deposited on top of the grating teeth, and the dimensions were chosen to give a resonance in the region of 1 to 2 MHz. The groove depth was in the range of 0.01", and it was found that the diamond saw fabrication technique used did not provide adequate precision. Consequently the quality factors realized were low (< 3000), and use of relatively shallower etched grooves at higher frequencies is clearly called for.

Since a sufficient condition for the existence of this type of surface wave is a periodicity of the conditions along the surface, another technique for trapping the wave at the surface is deposition of an array of metal strips.

Key words Resonator, Grating, Horizontal Shear, Interdigital Transducer, PZT, Lithium Niobate, Quartz.

## Introduction

In an earlier paper[1] the existence of a horizontally polarized shear (SH) surface wave on a corrugated substrate was demonstrated by virtue of the exact analogy between this elastic wave problem and the corresponding electromagnetic problem. An extensive literature exists for the latter case and the solutions given were found to be in good agreement with experimental results obtained for shear surface waves on a corrugated aluminum substrate. Observations were made by fabricating a finite length of corrugated surface (or grating) and measuring the transmission resonances with thickness shear transducers bonded to the ends of the finite length of grating. The surface nature of the wave was confirmed by measuring gratings on substrates of different depths.

Although previous experiments confirmed the applicability of the electromagnetic solutions to the elastic wave problem, the transducers used excited both the surface wave of the grating and thickness waves of the substrate. The mode spectrum was therefore cluttered with many spurious responses and entirely unsuitable for resonator applications. The present paper describes an investigation of SH surface wave resonances on piezoelectric substrates. Efficient selective excitation of the grating is then achieved by suitably choosing the substrate orientation and depositing a transducer electrode on top of each tooth. As will be seen, individual resonant modes of a finite length of grating may be excited by suitably chosing the distribution of voltages applied to the electrode array.

It should be pointed out that the SH surface wave considered here is intimately related to the surface-skimming shear wave.[2,3] The latter wave or, more properly, radiation pattern consists of a horizontally polarized shear elastic vibration skimming along the surface and slowly diffracting into the substrate. Diffraction losses are determined by the vertical directivity of the interdigital transducer (IDT) used for excitation. Consistent with the analogy of the IDT as an end-fire antenna array, the radiation pattern is sharpened and diffraction losses are reduced by increasing the length of the IDT. Addition of a grating structure to the surface permits the existence of a genuinely bound SH wave, which travels at a velocity slower than that of a bulk SH wave. If the IDT is suitably designed to synchronize with this bound wave, as in the case of a Rayleigh wave transducer, there will be essentially no diffraction loss into the substrate.

## SH Waves on an Infinite Grating

One way of picturing an SH grating vibration is to imagine it as evolving from the standard tuning fork resonator shown in the upper left of Fig. 1. An analogous type of tuning fork, in which the arms move in face shear, is shown on the right. Stacking of a number of these resonators in an array leads to the tuning fork grating shown at the bottom of the figure, in which the dashed lines are traction-free surfaces. The basic SH grating (Fig. 2) evolves from this as the dimension is extended to infinity along the particle displacement direction and the individual supports are replaced by a continuous substrate. With a fixed tooth spacing $d$, the frequency increases with decreasing length of the teeth, just as in the case of the original tuning fork. The grating configuration provides a means for realizing a tuning fork type of resonance at frequencies where a single fork becomes too small to fabricate and mount.

Because the spatial period of the vibration in Fig. 2 is $2d$ the displacement field in the substrate can be written as the Fourier series shown in the figure, where $a_n$ is the amplitude of the $n^{th}$ Fourier component and the Y exponential coefficient $\gamma_n$ is related to the wavelength of a bulk shear wave by the equation on the line below. It follows from this that $\gamma_n$ is real when $2d$ is less than a bulk shear wavelength. In this case all of the Fourier components decay exponentially into the substrate - that is, the motion is a surface vibration bound to the grating. This argument does not, of course, prove the existence of such a vibration, but its existence has already been demonstrated analytically in the case of the analogous electromagnetic problem.[4,5]

The vibration shown in Fig. 2, which has a phase shift of $\pi$ from one grating tooth to the next (the $\pi$-mode), is only one of many that can exist on this periodic structure. In the previous discussion, the grating was regarded as essentially an infinite array of tuning forks. Alternatively, one may look at the teeth as an array of cantilever supported face shear plate vibrators that are lightly coupled, one to the next, through the substrate. The vibration spectrum consists of a continuous distribution of coupled modes, analogous to the modes of a periodically mass-loaded vibrating string. In this case the phase shift from section to section is related to a continuous wave number $k = 2\pi/\lambda$, which takes the value $\pi/d$ for the $\pi$-mode discussed above (Fig. 3).

As shown in References 4 and 5 the relationship between $\omega$ and $k$ for this grating surface wave has the same form as for waves on the periodically loaded string. The frequency of the $\pi$-mode ($k = \pi/d$ in Fig. 3) corresponds to the lower edge of the stop band. Above this frequency the surface wave is nonpropagating (or cut-off). As the depth of the grating grooves is decreased, the frequency of the $\pi$-mode increases until the $V_{SHEAR}$ line is reached. This corresponds to the surface-skimming shear wave discussed above. In the so-called slow wave region below this line the solution is always a surface wave.

It should be emphasized that very little slowing is required to produce a well-confined surface wave. A Rayleigh wave, for example, has a phase velocity that is only some five percent below the bulk shear velocity but is confined to a depth less than a shear wavelength. One needs, therefore, only a shallow grating to trap the SH wave on the surface.

## Finite Grating Resonators

To produce a standing surface wave resonance the grating structure must be terminated in a pair of mirror reflectors. In the standard SAW resonator these mirrors are realized by long (several hundred periods) grating arrays designed to operate in the cut-off region. For the SH surface wave resonator this is not necessary. A mirror can be realized by terminating the grating in a suitably located traction-free boundary. In the case of the $\pi$-mode this is easily seen by examining Fig. 2, where the particle displacement is along $x$ and varies with $y$ and $z$. From the symmetry of the vibration one has that the displacement $u_x$ is maximum with respect to the $z$ variation at the plane denoted by a dashed line in the figure. This means that the strain component $S_{xz}$ and the stress component $T_{xz}$ are zero on this plane. Since $u_x$ is a function only of $y$ and $z$, the stress components $T_{yz}$ and $T_{zz}$ are also zero - just the conditions required for a traction-free boundary, which acts as a perfect mirror. By further symmetry arguments one can show that the same boundary conditions acts as a perfect mirror for a surface wave with any wavenumber $k$.

Figure 4 gives the profile of an $N$ section resonator contained between two such mirror reflectors. As in any standing wave resonance, the resonance condition is that the length $L$ be integral number $n$ of half wavelengths or, equivalently, that $k = n\pi/ND$. For a 10-section resonator there are therefore ten modes of resonance, with frequencies determined from the dispersion diagram by the construction shown on the figure. A particular mode may be excited by applying the corresponding distribution of voltages to the electrodes located on the tops of the teeth. Our experiments have been performed on the $\pi$-mode in which alternate electrodes are excited 180° out of phase, as in a conventional IDT.

We have fabricated and tested three SH grating resonators with groove profile dimensions as given in the upper left of Fig. 4 and resonant frequencies for the $\pi$-mode in the range of 1 to 2.5 MHz. The resonator proper is defined by an electroded region on the top surface of a grooved block, large enough to eliminate edge effects and to permit probing of the vibration pattern outside the electrode region by means of small rubber damping pads. The grooves were first cut with a diamond saw, the top surface and reflecting edges were then polished, the electrodes deposited and the gold wire leads attached.

In these initial experiments no attempt was made to polish the inside of the grooves. As will be seen, this leads to problems with resonance broadening and coupling into spurious modes due to grating nonuniformity and surface roughness. It is clear that the best way to make these structures is by deep etching techniques.[6]

The importance of groove depth uniformity is clear from the dispersion curves in Fig. 4, where it is seen that the frequency of the $\pi$-mode is strongly dependent on the groove depth $h$. Nonuniform groove depth therefore causes different parts of the grating to resonate at different frequencies. This effect was observed in some of our gratings, where the vibration was found by mechanical probing to be localized in a small region of the grating. Tighter tolerances on the fabrication procedure were found to reduce this effect. It appears from these results that the resonance could be confined to a desired region of the surface by deliberately tailoring the depth profile of the grooves.

Mechanical probing of the resonators with small rubber pads confirmed the surface wave nature of the vibration and also demonstrated a lateral confinement of the vibration to the electroded region. A lateral decay distance of the order of 1 cm was observed outside the electroded region. This is due to mass loading by the electrodes, which effectively increases the depth of the grooves under the electrodes. Because of this lateral confinement transverse modes are also observed, as in standard SAW resonators.

## PZT-8 Ceramic Resonator

The insert of Fig. 5 shows a highly schematic representation of the resonator geometry. Poling is in the direction indicated by the heavy arrow. Since it is not possible to pole over a 3" length, the block was fabricated from six 1/2" pieces carefully ground and bonded together with epoxy. No repolishing was performed after sawing the grooves, and the groove depth was measured to be approximately five percent greater at the left end of the grating than at the right. When the two halves of the grating were excited independently, different resonant frequencies were obtained - as expected, the lower frequency corresponding to the larger groove depth.

Figure 5 shows the measured input impedance characteristics for the entire grating - the small peak at 1.120 MHz corresponding to the deep end of the grating. A variation of groove depth in the order of five percent corresponds to a frequency variation in the order of one percent. The estimated resonator Q is of order 200, compared with a material Q of order 400 determined by pulse echo measurements in a large block.

We have also tested the same geometry as a Rayleigh wave grating resonator, with the poling in the vertical direction in Fig. 5. As anticipated the Q is much lower (of order 50) because traction-free boundaries do not act as good mirrors for Rayleigh wave motion.

## Y-X Lithium Niobate Resonator

A lithium niobate resonator was made in order to more clearly isolate the effects of surface roughness and resonator geometry on the Q-factor. As shown in Fig. 6 a resonator of somewhat different dimensions was made on a single crystal block, using the same fabrication method. The top surface is Y-oriented and the grooves are along Z . By cutting the grooves before polishing the top surface and finishing afterwards, grooves with clean upper corners were obtained. They were, however, very fragile and had to be handled with great care.

The impedance curve in the figure is for an unsupported sample and exhibits a very dense spectrum of spurious bulk modes in the region of the main and transverse surface wave resonances. Appearance of strong spurious modes only in the region of surface wave resonance indicates that the spurious coupling is through mechanical imperfections of the grating and not directly from the electrodes.

Figure 7 shows, on the same scale, the impedance characteristics after glueing the ends of the lithium niobate block. The bulk modes are now strongly suppressed, although some spurious is still apparent near to two transverse resonances on the high frequency side of the main resonance. There is now a strong surface wave resonance with a maximum impedance of 300 kΩ , and Figs. 8 and 9 show that the maximum spurious response over the range from 1 to 7.5 MHz is 4 kΩ .

Figure 10 gives on a logarithmic scale the detailed impedance response in the vicinity of the resonance and antiresonance points. Because of the large number of spurious modes near the series resonance point, it is not possible to calculate the Q by the standard procedure, but it is estimated to be not more than 2000. This very low value is clearly due to the energy loss coupled into a large number of bulk modes and subsequently dissipated in the supports. Further precision in grating fabrication is obviously called for.

## ST Quartz Resonator

Figure 11 shows the geometry of a grating resonator on a 39.3° "ST" quartz plate with the grooves along the X direction. Note that the thickness of the substrate is much less than in the other examples. Although the resonator is unmounted the spurious mode response is small compared with the lithium niobate case, and the response is clean outside the 10 KHz frequency range shown.

As in the PZT resonator the low frequency peak is attributed to nonuniformity of groove depth. Since this second peak occurs very close to the main series resonance point, it is not possible to arrive at an accurate evaluation of Q. We estimate a value in the order of 3000.

## Conclusions

In summary, we have experimentally verified the surface character of SH vibrations on deep grating structures and have measured some of the properties of grating resonators of this type operating on PZT-8, YX lithium niobate and ST quartz in the frequency range of ½ to 2 MHz. Q-factors obtained are low, not more than 3000. This is due in part to technical difficulties in accurately and uniformly fabricating the large grooves required at these low frequencies and in part to mode scattering due to the effect of substrate anisotropy on the behavior of the traction-free reflector surfaces.

The fabrication problems encountered point up the need to study shallower grating resonators operating at higher frequencies. As pointed out earlier, only a small amount of slowing is needed to trap the SH vibration on the surface, and the grooves need only be a small fraction of a wavelength in depth. Since the periodicity needed for wave trapping may also be induced by periodic boundary conditions on the surface, an attractive alternative is mass-loading or electrical short circuit strips deposited on the substrate surface.[7]

The major potential advantage of the SH grating resonator over the standard SAW structure is in its small size. Because the grating itself does not serve as a mirror, only a small number of periods is required. Also, the presence of a spectrum of resonator modes that can be selected by appropriate coding of the applied electrode voltages suggests the possibility of small multipole monolithic filters at very high frequencies.

## Acknowledgements

The authors wish to acknowledge the able technical assistance of W. Bond, L. Goddard, G. Kotler and D. Walsh.

This work was sponsored by the Joint Services Electronics Program under Contract N00014-75-C-0632.

## References

1. B. A. Auld, J. J. Gagnepain and M. Tan, Electronics Letters 12, pp. 650-651 (1976).

2. T. I. Browning and M. F. Lewis, these Proceedings.

3. K. H. Yen, K. L. Wang and R. S. Kagiwada, these Proceedings.

4. R. A. Hurd, Can. J. Phys. 32, pp. 727-734 (1954).

5. R. A. Collin, "Field Theory of Guided Waves," pp. 465-469, McGraw-Hill (1960).

6. C. A. Adams and J. A. Kusters, these Proceedings.

7. A. A. Oliner and A. Hessel, Trans. IRE AP-7, pp. 5201-5208 (1959).

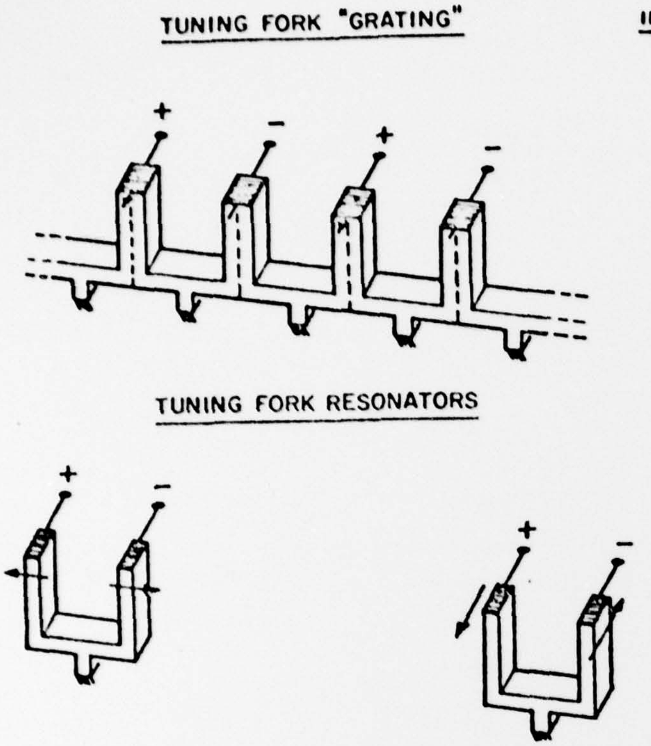


FIGURE 1. A Conventional flexural tuning fork resonator is shown in the upper left and a "face-shear" analogue in the upper right. The bottom of the figure shows a primitive horizintal shear grating resonator realized by stacking "face-shear tuning forks.

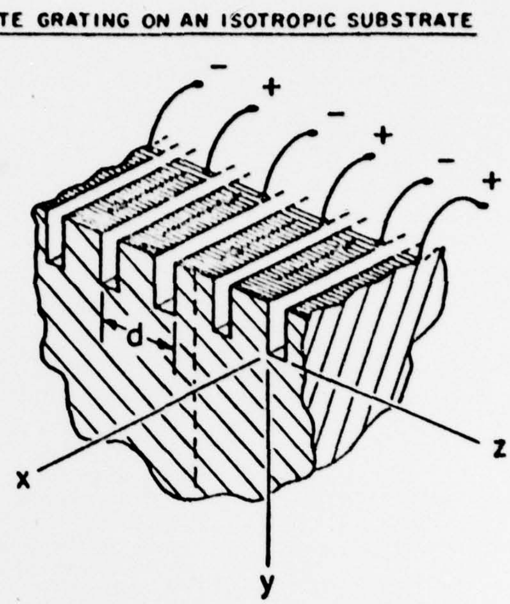


$$u_x(y,z) = \sum_n a_n e^{-\gamma_n y} e^{-i\frac{n\pi}{d}z}$$

$$-\gamma_n^2 = \left(\frac{2\pi}{\lambda_{SHEAR}}\right)^2 - \left(\frac{n\pi}{d}\right)^2 < 0$$

WHEN $d < \frac{\lambda_{SHEAR}}{2}$

$\Downarrow$

SURFACE VIBRATION

FIGURE 2. Horizontal shear grating on a semi-infinite substrate. Vibration is in the $\pi$-mode.

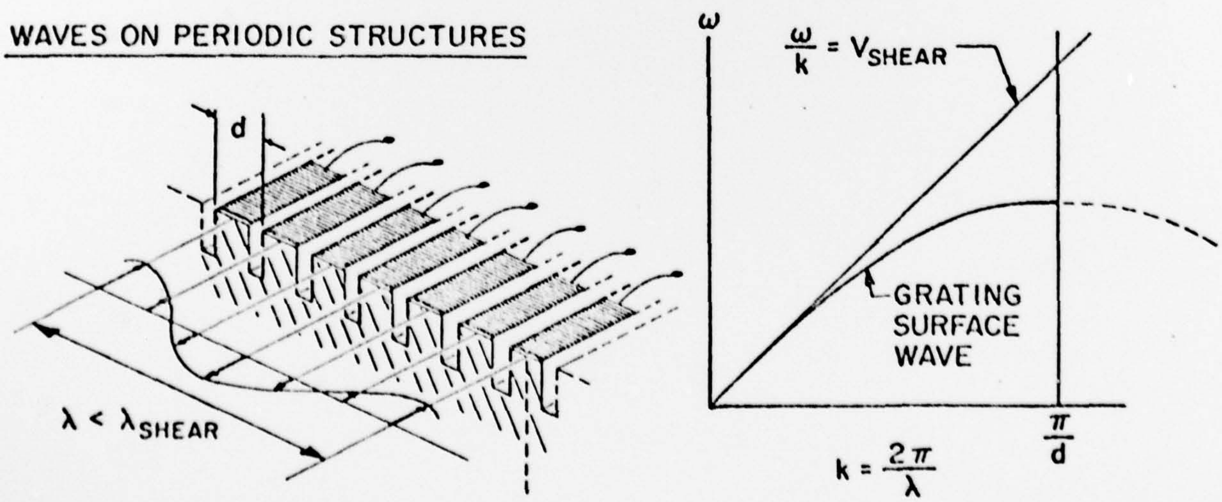


FIGURE 3. Typical form of the lowest branch of the dsipersion relation for the horizontal shear grating.

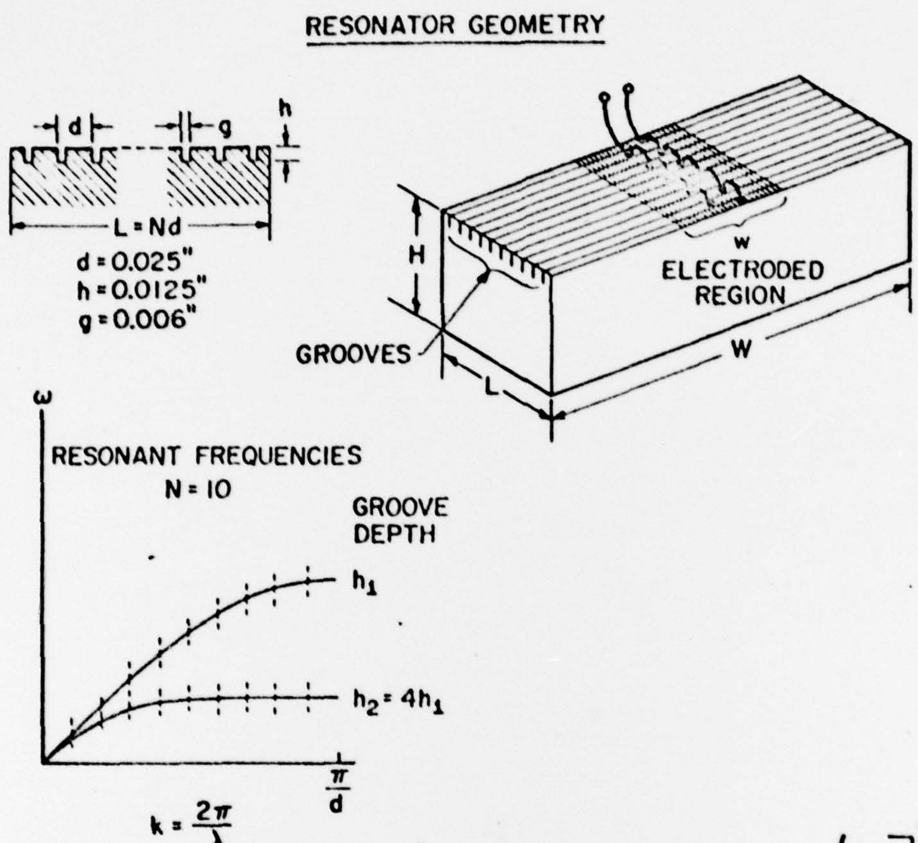


Fig. 4 Basic resonator structure and relationship between the dispersion relation and the resonant mode spectrum.

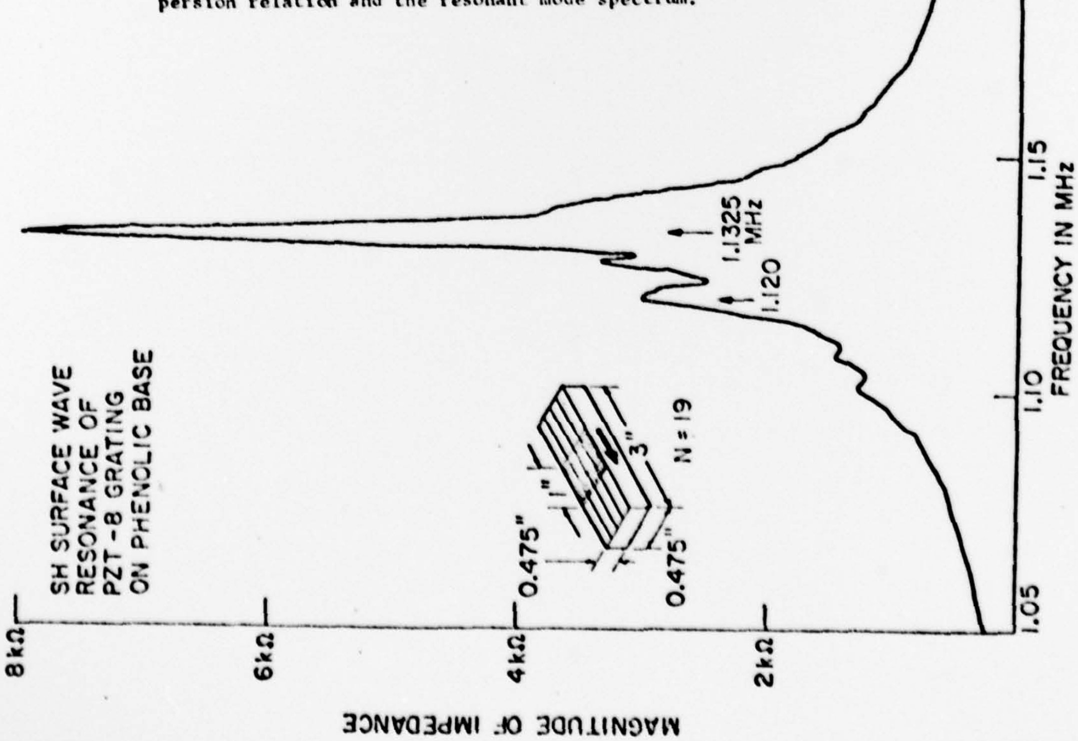


Fig. 5 Measured impedance-frequency curve of PZT-8 resonator. Poling direction is indicated by the heavy arrow.

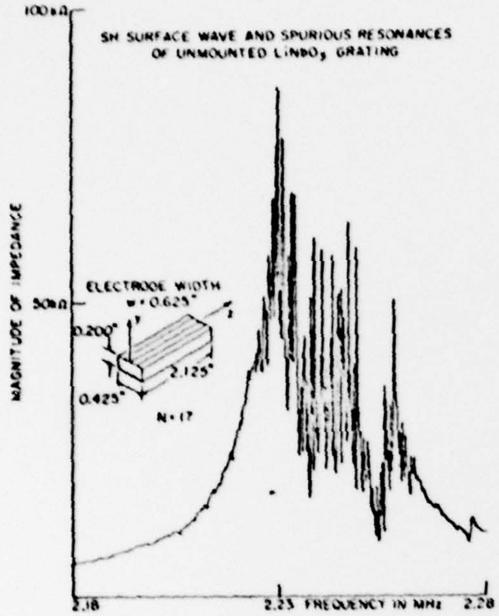


FIGURE 6. Impedance-frequency response of Y-oriented X-propagating $LiNbO_3$ grating resonator, showing a dense spectrum of spurious bulk resonances superposed on the main and trans-surface wave resonances. Area of the electroded region (not shown) is 0.425" X 0.625".

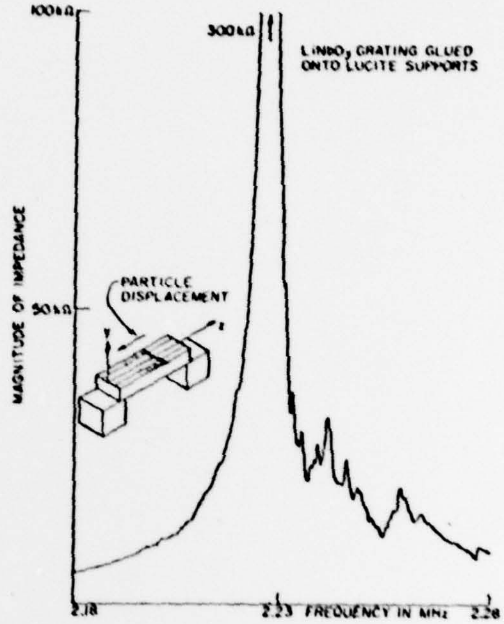


FIGURE 7. Same as Fig. 6, but with ends of the substrate glued to lucite supports. Note the two transverse mode resonances, with superimposed spurious resonances, on the high frequency side of the main resonance.

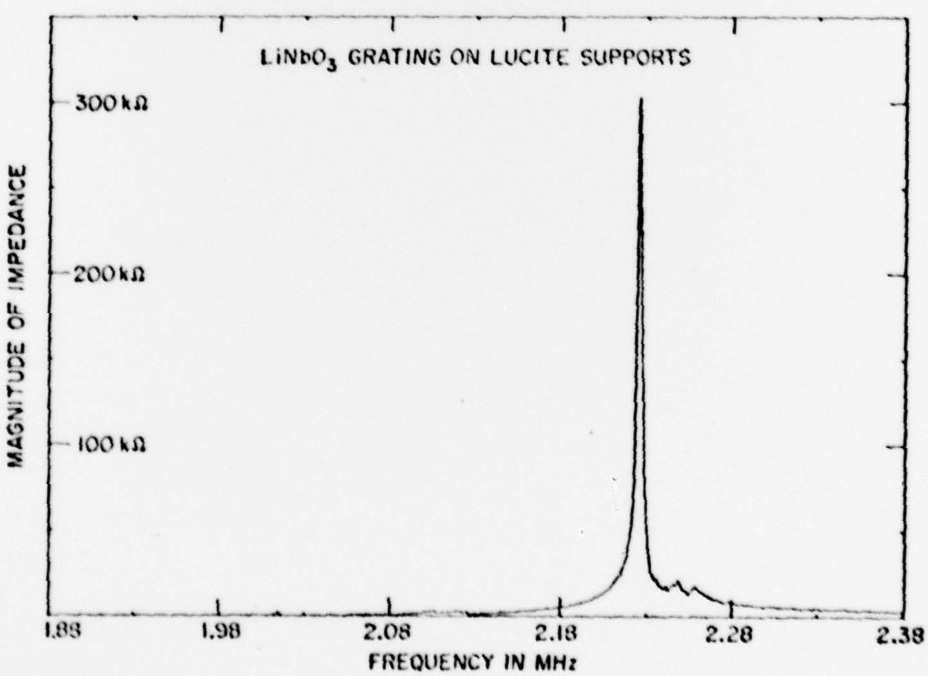


Fig. 8 Impedance-frequency curve of the $LiNbO_3$ grating, showing the peak of the main resonance and a wider portion of the skirts.

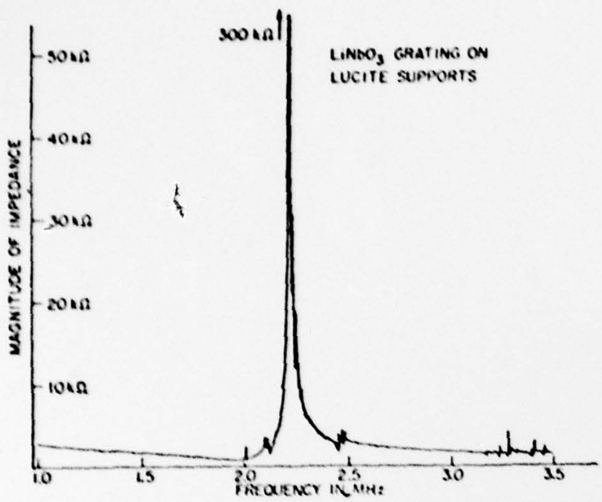


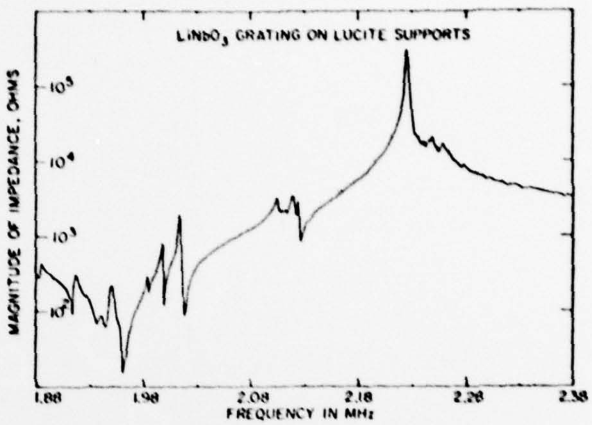


FIGURE 9. Illustration of the spurious mode response between 1 MHz and 3.5 MHz. Measurements out to 7.5 MHz showed a maximum spurious impedance peak of 4 kΩ over this frequency range.

FIGURE 10. Logarithmic impedance curve in the vicinity of the resonance and antiresonance points.

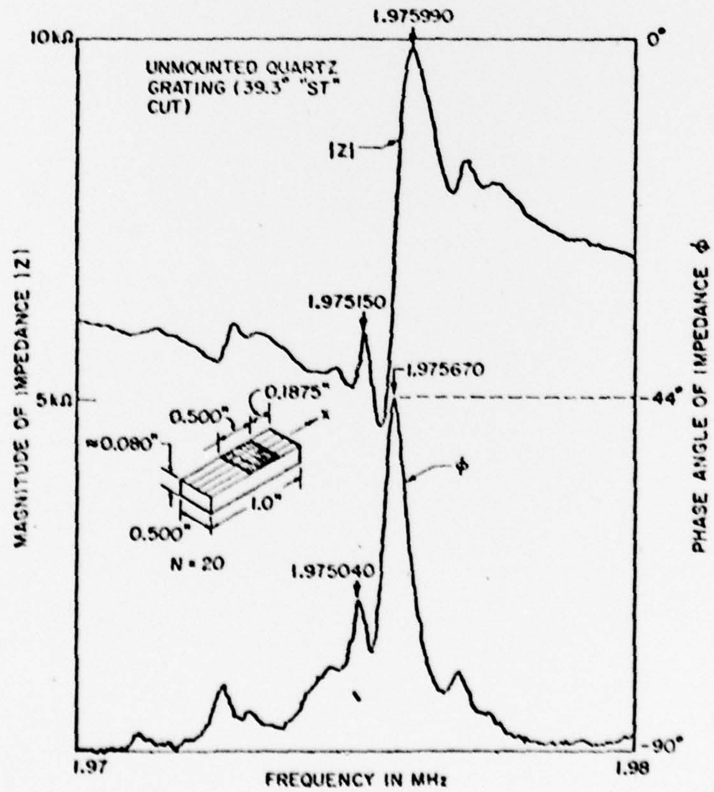


Fig. 11 Impedance-frequency curve of unmounted quartz grating on a 39.3° "ST" plate.